

# MESODAMAGE OF 2024-T3 ALUMINUM ALLOY SPECIMEN DUE TO CORROSION-INDUCED LOCALIZED HYDROGEN EMBRITTLEMENT

Al. Th. Kermanidis<sup>1</sup>, P. Papanikos<sup>2</sup> and Sp. G. Pantelakis<sup>1</sup>

<sup>1</sup>Laboratory of Technology & Strength of Materials, Department of Mechanical Engineering & Aeronautics, University of Patras, 26500 Patras, Greece

<sup>2</sup>Institute of Structures and Advanced Materials, ISTRAM, 57 Patron-Athinon Road, Patras 26441, Greece

## ABSTRACT

For the evaluation of the structural integrity of ageing aircraft components the effect of corrosion has to be accounted for. In recent years it has been recognized that corrosion of 2024-T3-aluminium alloy is associated to localized hydrogen embrittlement. Obtained damage is location, size, time and temperature dependent. Macroscopically it is reflected through a dramatic reduction of tensile ductility and fracture toughness. A mesodamage concept is adopted to provide the missing link between atomic-and macro-scale level. The proposed model is based on the assumption that different exposure times of thin specimens can yield for the average properties of a number of prospective meso-volumes at a certain distance from the corrosion attacked location of a real aircraft component. The reduction of fracture toughness was associated with the reduction of strain energy density obtained from tension tests of corroded and non-corroded specimens. It was shown that the developed model could be used to evaluate the fracture toughness of the corroded alloy and, thus, the residual strength of corroded aircraft component.

## KEYWORDS

Meso-damage, corrosion, hydrogen embrittlement, fracture toughness, aluminium alloys, aging aircraft.

## INTRODUCTION

Corrosion and the associated hydrogen embrittlement of high strength aluminium alloys present a major threat to the structural integrity of aging aircraft structures. The potential interaction of corrosion with other forms of damage such as a single fatigue crack or multiple site damage can lead to loss of structural integrity and catastrophic failure [1]. Numerous committees and international conferences have been organized [2-3] to ponder on the problem of material degradation in older aircraft and one important issue is corrosion [4-5]. Currently, corrosion and hydrogen damage mechanisms of aluminium alloys are far from being understood. Involved damage processes occur in atomic scale. Corrosion attack of aluminium alloys has been attributed to the complex process of oxidation [e.g. 1, 6]. Yet, it has been recognized that additionally to oxidation processes, hydrogen produced during the corrosion process may diffuse to the material interior and lead to hydrogen-metal interaction [e.g. 7]. The hydrogen trapping sites depend on the alloy system [7-14]. In [9] the determined embrittlement of the Al-Mg and Al-Zn-Mg aluminium alloy systems was explained as the result of the formation of magnesium hydrides on the grain boundaries. Yet, a dramatic embrittlement of the

alloys 2024 following exposure in several corrosive environments has been reported in [7, 10-12]; 2024 belongs to the Al-Cu system. The same behavior was observed for the 6013, 8090 and 2091 alloys as well. In [13] hydrogen trapping sites for the Al-Cu alloy 2024 are identified. Currently no reliable methodologies exist to link the corrosion and hydrogen damage processes which occur in atomic level to the macroscopic material properties, which are required for structural integrity calculations. In the present work a meso-damage approach is introduced to obtain the missing link between atomic-and macro-scale level. The location, size and time dependency of damage is accounted for. The approach is based on the simplification that different exposure times of thin large scale specimens can yield for the average properties of a number of prospective meso-volumes at a certain distance from the attacked area of a real aircraft component. The approach has been utilized to overcome the need for performing experiments on specimen size reduced to microns. The experiments were used to assess the significantly reduced values of fracture toughness and tensile ductility at meso-volumes lying ahead of the corrosion attacked surface. The investigation is carried out for the Aluminium alloy 2024-T3. The reduction of fracture toughness at meso-volumes is assessed from the reduction of strain energy density obtained from tension tests of corroded and non-corroded specimens.

## MESODAMAGE APPROACH

Corrosion is the result of complex oxidation processes at atomic scale. Hydrogen embrittlement is a diffusion controlled process and it is associated with the concentration and trapping of hydrogen at preferable trapping sites. The process takes place at atomic scale as well. The severity of the hydrogen damage depends on location and time. As such a process, embrittlement evolution in a thick specimen or component is linked to the concentration of hydrogen atoms, as shown typically in Figure 1. Distance zero in figure 1 represents the hydrogen source which is the corrosion attacked area (e.g. the tip of a crack at a rivet. The crack acts as hydrogen channel). Embrittlement reaches its maximum value at the surface layer, which is saturated with trapped hydrogen and decreases gradually with decreasing concentration of hydrogen.

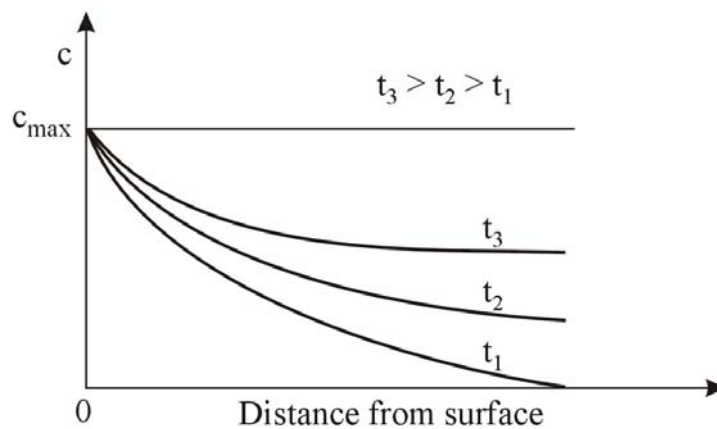


**Figure 1:** Hydrogen concentration along thickness for different exposure times (schematically)

This process may be interpreted as the embrittlement of three-dimensional meso-volumes, which exhibit different degree of embrittlement. It yields to varying mechanical properties and fracture toughness at the meso-level. The tensile tests described underneath can be used to evaluate these varying tensile properties and fracture toughness. In diffusion controlled processes same concentration of the diffusing medium can be achieved at short distances from the source of the diffusing medium and short diffusion times or at long distances from the source and long times. Thus, the properties of specimens subjected to different exposure times can be interpreted to reflect the average properties of a number of prospective meso-volumes at different distances from the surface. Early experimental results [5, 14] indicate that hydrogen diffusion is very low from the front and back surface of the specimens and high from the edges and through the thickness cuts. Obviously the specimen thickness of 1,6mm is too large as compared to the size of meso-volumes typically not exceeding a few microns. Yet, as shown in [14] the hydrogen may diffuse at distances larger than 25mm. Thus, the properties of the meso-volumes lying along the path of hydrogen diffusion may

be approximated through prospective average values derived each time for a number of meso-volumes involved in 1.6mm distance. With regard to the diffusion controlled embrittlement process the varying degree of embrittlement at different distances from the hydrogen source may be simulated through the exposure of specimens of same thickness (here 1,6mm) for different times at same corrosive environment.

## EXPERIMENTS

The experiments included firstly the exposure of specimens to corrosive environments as they are specified in the respective standards for accelerated laboratory corrosion tests for a number of different exposure times. Then the corroded specimens were subjected to mechanical testing.

### *Materials and Specimen Preparation*

The investigation was performed on the aluminium alloy 2024-T3 with the following chemical composition: 0.10% Si, 0.18% Fe, 4.35% Cu, 0.67% Mn, 1.36% Mg, 0.02% Cr, 0.07% Zn, 0.03% Ti, 0.01% Zr. The alloy was received in sheet form of 1.6mm nominal thickness. Tensile and fracture toughness specimens were prepared. Tensile specimens were machined according to ASTM E8m-94a; specimens were cut in both longitudinal (L) and long transverse (LT) direction. Fracture toughness specimens were cut in (L) direction following the ASTM E561-94 specification. More details about the corrosion tests can be found in [12].

### *Mechanical Testing*

The tensile tests aim to provide information on the gradual decrease of the tensile properties during exfoliation corrosion exposure and to assess the degree of properties with increasing distance from the hydrogen source. All tensile tests were performed according to ASTM E8m-94a specification using a 200 KN Zwick universal testing machine and a servohydraulic MTS 250 KN machine by a deformation rate of 10 mm/min. Fracture toughness tests were conducted according to the ASTM 561-94 specification.

## RESULTS AND DISCUSSION

### *Mechanical Characterization*

The tensile properties of the reference material are summarized in Table 1. The energy density is evaluated by the area under the true stress-strain curve.

TABLE 1  
TENSILE PROPERTIES FOR REFERENCE MATERIALS

Material	Yield stress, $S_y$ (MPa)		Ultimate tensile stress, $R_m$ (MPa)		Elongation to failure, $A_{50}$ (%)		Energy density, $W$ (MJ/m <sup>3</sup> )	
	L	LT	L	LT	L	LT	L	LT
2024-T3	396	339	520	488	18.0	18.0	86.7	81.7

The residual mechanical properties as a percentage of the properties of the reference material are shown in Figure 2 for the L (a) and LT (b) directions. The figure shows the property decrease trend versus exposure time in exfoliation corrosion solution. All properties decreased non-linearly with exposure time. It is clear from Figure 1 that yield and ultimate tensile stress have been practically not affected. On the contrary, a clear trend of an appreciable tensile ductility decrease has been observed. Obtained yield and ultimate tensile stress decrease is caused by corrosion induced material surface degradation. It was found that after machining of the corrosion attacked material surface layer, yield and ultimate tensile stress increase again almost to their initial values. Yet, tensile ductility drop is volumetric. Machining of the corrosion attacked surface layer had practically no influence on the determined tensile ductility values although the tensile tests were performed on the “non-corroded” material core after the removal of the corrosion-attacked layer. In [13], the observed bulk embrittlement has been associated to hydrogen penetration and absorption.

## Fracture Toughness

Figure 3 shows the fracture surfaces of a non-corroded (a) and a corroded fracture toughness specimen (b). It is clear from the figures that the mode of final failure is different for the two cases. In the non-corroded specimen, a typical ductile fracture is observed. However, a brittle fracture is observed in the corroded specimen indicating that the corrosion-induced embrittlement goes far beyond the corroded layer of the material, which for the specimen showing in Figure 3(b) has a depth of 200  $\mu\text{m}$ . The failure surface indicates the gradual change from a brittle to a ductility failure with increasing distance from the corroded area. Table 2 shows the fracture toughness tests conducted and the values of fracture toughness obtained. For the case of protected specimens (anodizing and sealing), no corrosion effect was observed. The small decrease of the fracture toughness as compared to the un-protected reference specimens might be attributed to the fact that the process of anodization leads to material embrittlement. The results for the un-protected specimens indicate that corrosion leads to a significant decrease in fracture toughness (27%). Yet, the dimensions of the specimen are by far larger as the distance within hydrogen may diffuse. Obtained fracture toughness values reflect specimens which are partially fully embrittled, in certain locations only partially embrittled to different degrees of embrittlement and, far from the hydrogen source, not embrittled at all. The approach described underneath will be utilized to yield to local fracture toughness values. Following to the work in [15], the strain energy density evaluated from the stress-strain curve of the material can be associated to the fracture toughness with the relation:

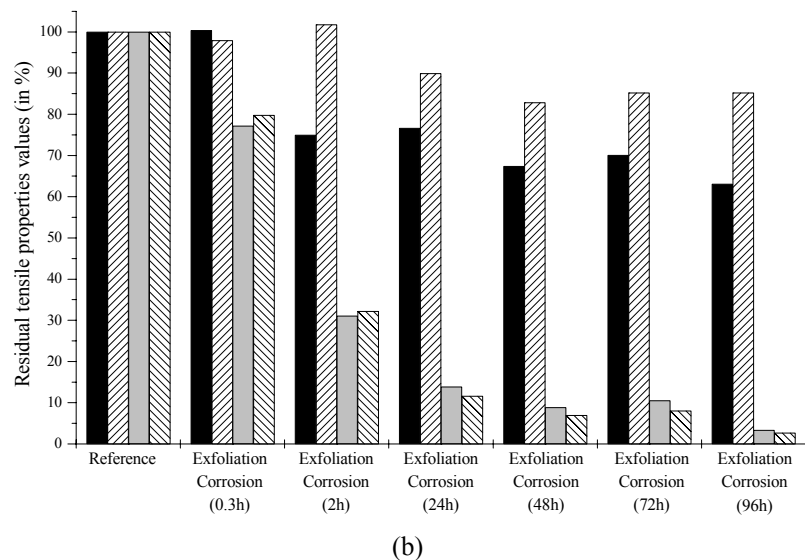
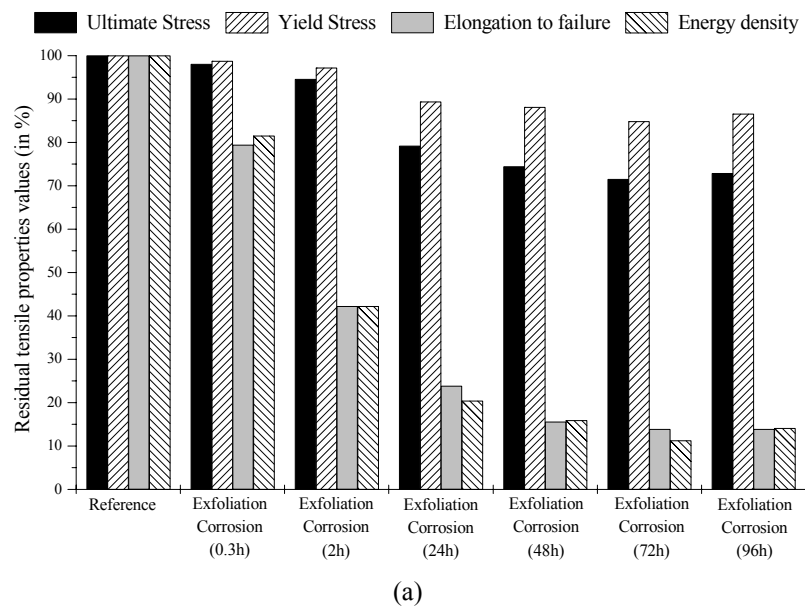


**Figure 2:** Gradual tensile property degradation for the alloy 2024 during exposure in exfoliation corrosion solution: (a) L direction, (b) LT direction.

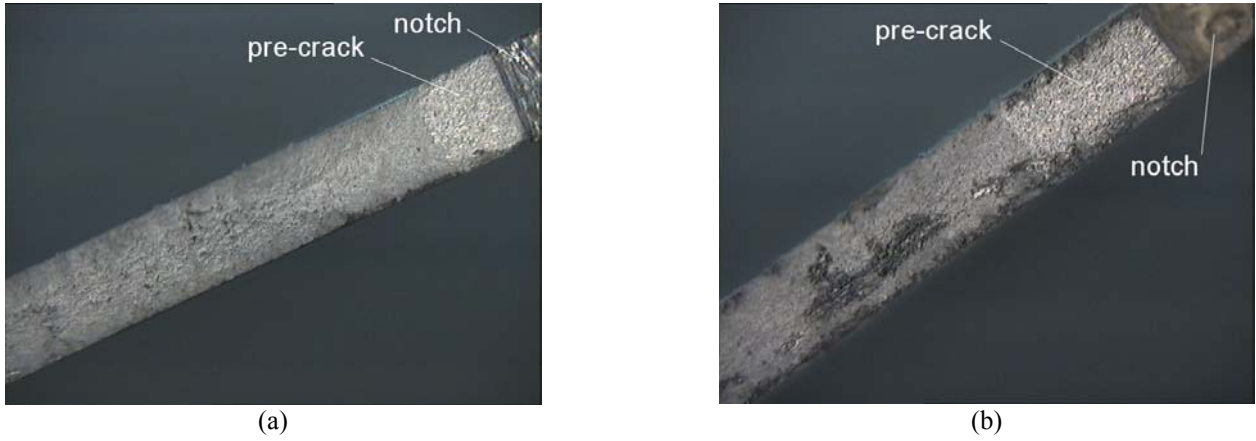


**Figure 3:** Fracture surfaces of a (a) non-corroded and (b) corroded (EXCO 36 h) fracture toughness specimens

TABLE 2  
FRACTURE TOUGHNESS TEST RESULTS

Material 2024-T3	Corrosion exposure	Direction/ number of tests	$K_c (MPa\sqrt{m})$
Reference	None	L/2	134.6
Corroded	EXCO 36 h	L/2	97.8
Reference (anodized and sealed)	None	L/2	126.5
Corroded (anodized and sealed)	EXCO 36 h	L/2	125.2

$$K_c^2 = \beta W \quad (1)$$

where  $K_c$  is the fracture toughness,  $W$  the strain energy density and  $\beta$  a function of the elastic properties of the material. The quantity  $\beta$  will be considered constant with corrosion exposure. Eqn. 1 can be used to estimate the value of  $K_c$  for an embrittled material due to corrosion since it suggests that

$$K_c^2(cor) / K_c^2 = W(cor) / W \quad (2)$$

Using the values of Table 1 and the results of Figure 1(a) it can be estimated that the value of energy density for 36 h exfoliation corrosion is  $W(36h) = 14.7 MJ/m^3$ . From Tables 1 and 2 we have that  $K_c = 134.6 MPa\sqrt{m}$  and  $W = 86.7 MJ/m^3$ . Therefore, Eqn. 2 gives  $K_c(36h) = 55.4 MPa\sqrt{m}$ . This value is however much smaller than the measured value of  $97.8 MPa\sqrt{m}$ . The reason for this discrepancy is that the fracture toughness specimen does not experience volumetric embrittlement as the tensile specimen used to obtain the strain energy density. The above observation is very important as far as the structural integrity of a corroded aircraft structure is concerned. It indicates that the use of the virgin material fracture toughness for assessing the structural integrity of aged and corroded components may result to essential overestimation of residual strength, which could lead to fatal consequences. On the other hand, the use of the value of fracture toughness evaluated assuming volumetric embrittlement of the material can be very conservative and lead to over sizing. It is therefore necessary for a specific problem to use a local fracture toughness, which will range from the minimum value (volumetric embrittlement) to the maximum value of the virgin material. This is especially true for MSD problems where the distance of the rivet holes is such that allows local volumetric embrittlement of the material. This work is currently extended to investigate this issue.

## CONCLUSIONS

A mesodamage concept is proposed to evaluate the location, size and time dependent embrittlement as a result of hydrogen diffusion and trapping during the corrosion process. The investigation was carried out for the Aluminium alloy 2024-T3. The work indicates the following:

- Corrosion-induced degradation of mechanical properties occurs gradually with the exposure time or the distance from the attacked surface. Tensile ductility decreases exponentially to extremely low final values.
- Tensile test results can be used to evaluate the varying material properties and fracture toughness of a component at any depth and level of embrittlement.
- The fracture toughness of the corroded material decreases significantly. It is necessary to evaluate a local fracture toughness associated with the reduction of strain energy density.
- Adoption of the proposed mesomechanics approach has been proven very efficient for facing the complex interactive corrosion-hydrogen embrittlement process.

## ACKNOWLEDGMENTS

This work was partially supported by the Greek General Secretariat for Research and Technology (project PENED99 /649).

## REFERENCES

1. Inman, M.E., Kelly, R.G., Willard, S.A. and Piascik R.S. (1997). In: *Proceedings of the FAA-NASA Symposium on the Continued Airworthiness of Aircraft Structures*, pp. 129-146, Springfield, Virginia.
2. FAA-NASA Symposium on the Continued Airworthiness of Aircraft Structures, FAA Center of Excellence in Computational Modeling of Aircraft Structures, Atlanta, USA, 1996.
3. AGARD Workshop, *Fatigue in the Presence of Corrosion*, RTO Meeting Proceedings 18, Corfu, Greece, 1999.
4. BRITE/EURAM 1053, Structural Maintenance of Aging Aircraft (SMAAC), CEC Brussels, Final Report, 1999.
5. EPETII/30 (1999). *Damage Tolerance Behavior of Corroded Aluminum Structures*. Final Report, General Secretariat for Research and Technology, Greece.
6. Smiyan, O.D., Koval, M.V. and Melekhov, R.K. (1983) *Soviet Mater. Sci.* 19, 422.
7. Pantelakis, Sp.G., Vassilas, N.I. and Daglaras, P.G. (1993) *Metall* 47, 135.
8. Scaman, G.M., Alani, R. and Swann, P.R. (1976) *Corrosion Science* 16, 443.
9. Tuck, C.D.S. (1980). In: *Proceedings of the 3<sup>rd</sup> Int. Conference of Hydrogen on the Behavior of Materials*, pp. 503-510, Jackson, USA.
10. BRITE/EURAM BE92-3250, Investigation on Aluminium-Lithium Alloys for Damage Tolerance Applications, Final Report, CEC Brussels, 1993.
11. Pantelakis, Sp.G., Kermanidis, Th.B., Daglaras, P.G. and Apostolopoulos, Ch.Alk. (1998). In: *Fatigue in the Presence of Corrosion*, AGARD Workshop, Corfu, Greece.
12. Pantelakis, Sp.G., Daglaras, P.G. and Apostolopoulos, Ch.Alk. (2000) *J. Theor. Appl. Fract. Mech.* 33, 117.
13. Haidemenopoulos, G.N., Hassiotis, N., Papapolymerou G. and Bontozoglou V. (1998) *Corrosion* 54, 73.
14. PENED99/649 (2000). *Corrosion and Hydrogen Embrittlement of Aircraft Aluminum Alloys*. Mid Term Assessment Report, General Secretariat for Research and Technology, Greece.
15. Jeong, D.Y., Orringen, O. and Sih, G.C. (1995) *J. Theor. Appl. Fract. Mech.* 22, 127.